Pergamon

Energy Convers. Mgmt Vol. 37, No. 11, pp. 1589–1599, 1996

S0196-8904(96)00002-7
0196-8904/96 $15.00 + 0.00

DIGITAL COMPUTER COMPUTATION AND ANALYSIS OF GAS INSULATED SUBSTATION OVERVOLTAGES

ABDEL-SALAM H. A. HAMZA† and NAGAT M. K. ABDEL-GAWAD

Faculty of Engineering, Shoubra, Zagazig University, Cairo, Egypt

(Received 21 March 1995; received for publication 2 January 1996)

Abstract—A gas insulated substation can be subjected to a high amplitude of overvoltages as a result of lightning strokes striking the substation. This can cause a back flashover failure, which will damage the equipment and devices in the substation if these overvoltages are allowed to exceed those that the devices can withstand. In this study, an investigation of the overvoltages in a gas insulated substation as a result of a back flashover, with the variation of some different parameters, is conducted using a digital computer so that the substation performance can be determined under these conditions. This is very useful for determining the protection level and method of the gas insulated substation. Copyright © 1996 Published by Elsevier Science Ltd

Electrical power systems Gas insulated substation Lightning Back flashover Overvoltages

NOMENCLATURE

GIS = Gas insulated substation
CVT = Capacitive voltage transformer
C_T = Transformer capacitance
U = Busbar voltage
BIL = Basic Impulse Withstand Level

1. INTRODUCTION

Overvoltages can be produced in electrical power systems as a result of lightning surges. This is one of the main causes of electrical power transmission systems failures. For explanation of the nature and the cause of lightning, there are different theories of charge formation in clouds [1, 2] and how the lightning discharge occurs [3]. The methods for measuring lightning storms and description of the characteristics of lightning strokes are given in Ref. [4]. The effects of a lightning stroke on high voltage lines can be observed using a cathode-ray oscillograph. If a lightning surge wave which travels along a line struck by lightning was not mutilated by a flashover or modified by reflections, it has a simple wave shape. The wave shape can be specified by four characteristics, the crest, the front, the tail and the polarity of the wave [4]. A lightning surge wave can be represented mathematically by writing it as a summation of two exponential curves [4, 5];

$$e = E(\epsilon^{-\alpha t} - \epsilon^{-\beta t}). \tag{1}$$

From this equation, the crest value occurs when

$$\frac{\mathrm{d}e}{\mathrm{d}t} = E(-\alpha\epsilon^{-\alpha t} + \beta\epsilon^{-\beta t}) = 0. \tag{2}$$

The time value, therefore, has a relation as:

$$t = t_i = \frac{\ln\left(\frac{\beta}{\alpha}\right)}{\beta - \alpha} = \frac{1}{\alpha}\frac{\ln\left(\frac{\beta}{\alpha}\right)}{\left(\frac{\beta}{\alpha}\right) - 1} = \left(\frac{\mathrm{B}}{\alpha}\right). \tag{3}$$

†To whom all correspondence should be addressed at: Yanbu Industrial College, P.O. Box 30436, Madinat Yanbu El-Sinaiyah 21477, Kingdom of Saudi Arabia.

The crest value, therefore, has a relation as:

$$E_i = E(\epsilon^{-\alpha t_i} - \epsilon^{-\beta t_i}) = E(\epsilon^{-B} - \epsilon^{-B(\beta/\alpha)}). \tag{4}$$

The lightning surge specification can be determined by using another method, this is by using the values given in Table 1 [5].

1.1. Travelling waves and Bewley Lattice Diagram [*4, 6*]

When an electrical source is connected to a transmission line, the voltage does not appear immediately in it because there are distributed line capacitances. The voltage wave that travels along the transmission line suffers attenuation and distortion as energy losses exist and there are variations in the inductances and capacitances. If attenuation and distortion do not exist, the waves are propagated with the equations as follows:

$$U = F_1(x - vt) + F_2(x + vt) \tag{5}$$

$$I = \frac{F_1(x - vt) + F_2(x + vt)}{Z_0} \tag{6}$$

where U = voltage, I = current, x = the distance measured along the line, v = velocity of propagation and t = time. These two components are dependent on the reflection and refraction (transmission) coefficients K_R and K_T which can be written as:

$$K_R = \frac{Z_c - Z}{Z_c + Z} \tag{7}$$

$$K_T = \frac{2Z_c}{Z_c + Z} \tag{8}$$

where

$$K_R = K_T - 1. \tag{9}$$

Based on the reflection and refraction of travelling waves, Bewley proposed a graphical method (Bewley Lattice Diagram method) for calculating the variation of voltage at any point in cables or long lines at any time. This method can be used easily when the system is simple. However, in large systems in which many components are involved, using the Bewley Lattice Diagram is not practical. Bickford and Doepel and others have solved this difficulty. They have used the Bewley Lattice Diagram with a digital computer so that the voltage can be calculated accurately at any point at any time in a large system. This can be done by using the branch time-table [6]. The branch time-table is the heart of the Bewley Lattice Diagram and its digital computation.

1.2. Arrester for protection against overvoltages [*4, 7–12*]

Overvoltage may be caused at the substation and damage devices resulting from a lightning surge wave travelling to the substation. To prevent this bad situation, the overvoltage should be limited so that, in the protected area, the overvoltage can be maintained within acceptable values, i.e. below the insulation strength of the devices. Voltage limitation at the devices can be provided by the application of surge arresters. Surge arresters, which can be used for the protection, are one of two types.

(1) *The conventional arresters* [7, 11], which are most widely used on EHV and UHV power systems, are current limiting types. These consist of spark gaps and valve blocks, and the valve blocks are made of silicon carbide. The gaps sparkover during the overvoltage condition and the valve blocks control what happens afterwards, reducing the duty of the block by developing a back voltage provided by the gaps. The current flow is, thus, reduced to zero. The valve block can be represented by the equation:

$$\hat{U} = a_0 + a_1\hat{I} + a_2\hat{I}^2 \tag{10}$$

where

$$\hat{U} = \ln U$$

$$\hat{I} = \ln I; \text{ and } a_0, a_1, a_2 = \text{constants;}$$

and the voltage–current characteristic of the gap follows the relation:

$$\bar{U} = 1 + A(1 - \bar{I})^2 + B(1 - \bar{I})^4 \tag{11}$$

where $\bar{U}$ and $\bar{I}$ are the maximum gap voltage in p.u. of the gap voltage peak and the arrester current in p.u. of current at the gap voltage peak.

(2) *The gapless arrester* uses a zinc oxide non-linear resistor in which the air gap has been eliminated. For this study, the conventional type is applied.

2. SYSTEM TO BE STUDIED

The system to be studied and analyzed, as shown in the circuit diagram in Fig. 1 [13], is a transmission line which is connected to a gas insulated substation (GIS) and has some essential features. The average bus run for a compact GIS is much less than the one for a conventional station. Also, the GIS is free from any atmospheric contamination because it is totally enclosed. Further, the number of lightning arresters required is less than that of a conventional substation. Furthermore, its surge impedance is lower than that of the overhead lines. This makes the overvoltages in it lower. From these features, the GIS has become a serious competitor where atmospheric problems are severe and land cost is high. The GIS seems to be an automatic choice to be placed inside buildings in big cities or underground.

In this study, the system shown in Fig. 1 has been investigated for its lightning overvoltages performance. Overvoltages at a transformer (point 4), caused by a lightning stroke at the top of the 2nd tower (point 6) that results in a back flashover, will be observed when a lightning arrester having particular characteristics is connected at the entrance of the GIS (point 3). The overvoltages have also been investigated by varying the values of the capacitor voltage transformer (CVT) for measuring purposes, the length of the GIS trunk (the length between points 3 and 4) and the capacitance of transformer C_T. From these investigations, acceptable values for CVT, C_T, and GIS trunk length can be determined for design purposes.

3. DATA USED FOR THE STUDY

The important data required for the calculation using the computer program are:

(1) *Base voltage*, where voltages are represented in per unit (p.u.) value of voltage between line and neutral. A voltage of a transmission line of 400 kV is chosen as the voltage reference.

(2) *Busbars*. In the system, 8 (three-phase) busbars are used. A busbar consists of three individual phase busbars.

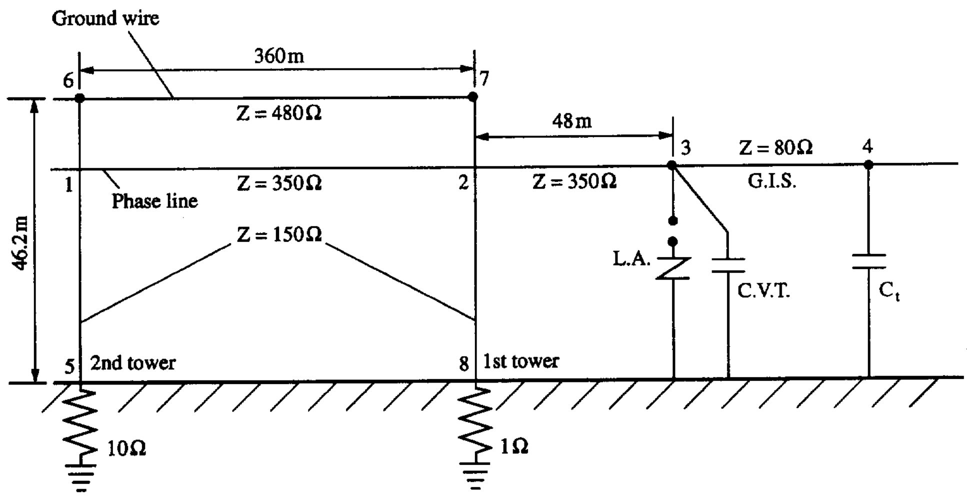

Fig. 1. A single line diagram of a transmission line and a GIS.

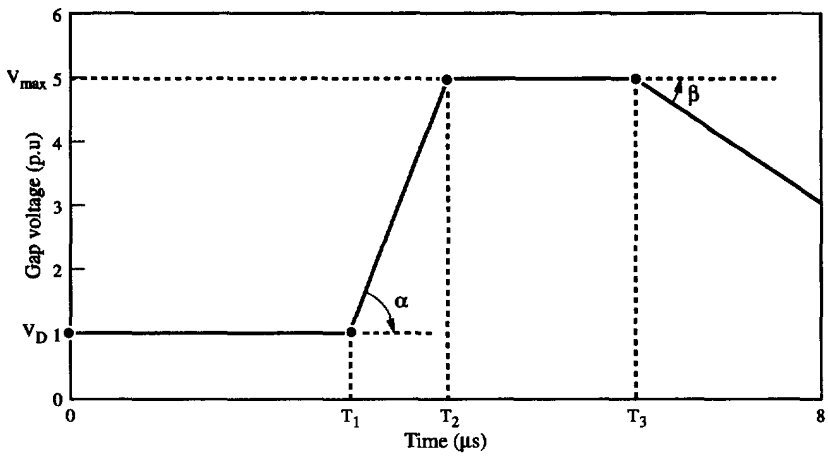

Fig. 2. Voltage–time characteristics of a current limiting gap (for gap arrester).

(3) *Single circuit transmission lines*, where a transmission line is specified by its sending and receiving end busbars, its length and surge impedance matrix. The assumptions chosen for calculation are no mutual impedances and no attenuation and distortion in transmission lines. The velocity of wave propagation is taken equal to the value of the velocity of light in air which is 300 m/μs.

(4) *Shunt capacitances*. One is for transformer representation in a short time transient and the other is a capacitor voltage transformer which is used for measuring purpose.

(5) *Shunt resistances data* required are similar to that for surge impedances in that both are assumed to have no mutual effects. The number of shunt resistances is two, one at the 1st tower base and the other at the 2nd tower base.

(6) *Arrester*. A conventional active gap arrester is applied at the entrance of the GIS. The 80% arrester rating is used with the section rating of 6 kV. The voltage–time characteristic of this arrester is in Fig. 2, where $T_1 = 400\ \mu$s, $T_2 = 900\ \mu$s, $T_3 = 1100\ \mu$s and $U_D = 2.2$ p.u. The valve of the arrester is simulated by a block characteristic which has constants, $a_0 = 5.2698$, $a_1 = 0.83374$, and $a_2 = -0.042453$.

(7) *The initial voltage conditions*, given to busbars in the phase lines, are 1.0 p.u. for voltage, 50 Hz for frequency, and 90°, −30° and 210° for phase angles in phases A, B and C, respectively.

(8) *The flashover level* across the insulator is taken as 3 p.u. [12] for 400 kV transmission lines. In the computer program calculation, flashovers are supposed to occur at the second tower from the GIS. To represent appropriately the flashovers, a three phase switch is applied between busbars 6 and 1, in Fig. 1, at time = 0 μs. Further, three resistances with very high values are connected between the switching busbars.

(9) *The lightning surge wave* applied is the one which has a wave shape 1/50. The value of 3 MV/μs is taken as its rate of rise. Therefore, the crest value is 7.5 p.u.

(10) *The value of the basic time interval* (θ) [7], $\theta = 0.01\ \mu$s is chosen throughout the calculations. The time of interest of the final time is 10 μs. The behaviour of the GIS that will be investigated

Table 1. Lightning surge parameters

Wave shape	E (p.u.)	α $(\mu s)^{-1}$	β $(\mu s)^{-1}$	Actual time to peak (μs)
0/1	1.0	0.6931	∞	0
0/5	1.0	0.1386	∞	0
0/50	1.0	0.01386	∞	0
0/100	1.0	0.000693	∞	0
1/5	1.81	0.253	1.35	1.52
1/50	1.036	0.0146	2.56	2.029
1.2/50	1.035	0.046	2.61	1.575
1/∞	1.0	0.0	2.746	∞

Table 2. Comparison of data calculated between GIS with and without CVT in back flashover where GIS trunk length = 40 m

	No CVT				CVT = 0.005 μf			
Busbar	Time for 1st wave (μs)	Voltage at 1st wave (p.u.)	U_{min} abs. (p.u.)	U_{max} abs. (p.u.)	Time for 1st wave (μs)	Voltage at 1st wave (p.u.)	U_{min} abs. (p.u.)	U_{max} abs. (p.u.)
6	0	0	0.1758	3.987	0	0	0.147	3.987
1	0.154	0.499	0.3783	3.193	0.154	0.4990	0.3701	3.228
3	1.52	0.4536	0.0231	2.096	1.52	0.4996	0.3228	2.187
4	1.66	0.4448	0.2069	2.356	1.66	0.4985	0.1696	2.803
5	0.154	—	—	—	0.154	—	—	—
7	1.20	—	—	—	1.20	—	—	—

is its performance under a lightning stroke at the second tower with a steep front of 1.0 μs. It is assumed that the maximum voltages which will exist in each point of the circuit are within 10 μs duration. However, the final time chosen for the calculation is 30 μs in order to observe the behaviour after 10 μs.

4. THE INVESTIGATION AND RESULTS

4.1. System circuit diagram

A lightning wave having a crest value 3000 kV (=7.5 p.u.), rate of rise 3 mV/μs and 1/50 waveshape is applied at busbar 6 of Fig. 1. From Table 1, the value of E is found, then the equation of the lightning wave can be represented as:

$$e = 7.77(\epsilon^{-0.0146t} - \epsilon^{-2.56t}).$$

It has been mentioned that the speed of wave propagation equal to the light velocity in air (300 m/μs) is used throughout the calculation. This value is equivalent to the propagation time of 3.336 μs/km. A correction must be given in the length of the GIS trunk because the wave propagation in the GIS is 330 m/μs [14]. The propagation time in the GIS then can be found equal to 3.03 μs/km. The actual length of the GIS trunk is then calculated as the GIS trunk used in the calculation multiplied by a factor 330/300.

4.2. Calculation of propagation times

The propagation times between busbars are calculated as follows:
busbar 6 to busbar 5, $t_{6-5} = (46.2/1000) \times 3.336 = 0.154\ \mu$s;
busbar 1 to busbar 3, $t_{1-3} = [(360 + 48)/1000] \times 3.336 = 1.361\ \mu$s,
busbar 3 to busbar 4 depends on the length of the GIS trunk. For a trunk length of 40 m, the time is $t_{3-4} = (400/1000) \times 3.336 = 0.1334\ \mu$s.

4.3. Voltage–time characteristics

From the output of the digital computation given in Table 2 and Figs 3 and 4, it is found that, when the lightning, with its specifications previously described, strikes the second tower (or busbar 6), the voltage at this bus bar increases rapidly, following the rate of rise of the lightning surge wave. As a result, there is a lightning surge wave transmitted through the ground wire and tower. At the tower base, the wave is reflected with the coefficient of reflection, $K_R = (10 - 150)/160 = -0.875$. The reflected wave has a negative sign. Before it reaches the tower, at 0.154 μs after the lightning has been applied, the voltage differences between busbars 6 and 1 in both phases B and C are greater than 3.0 p.u., which is the value the insulator can withstand. However, the voltage difference in phase A is less than 3.0 p.u. It is obvious from these facts that, at 0.154 μs, flashover only occurs at the insulators in phases B and C. The reflected wave from the tower base reaches the top of the tower at 0.08 μs, when the voltage differences between busbars 6 and 1 are phase A = 2.9866 p.u., phase B = 3.002 p.u. and phase C = 3.002 p.u. Again, flashover only occurs at phases B and C.

When flashover occurs, there is a travelling wave propagated from busbar 1 to the GIS. The negative reflected wave from the tower base reduces sharply the voltages of phases B and C at both

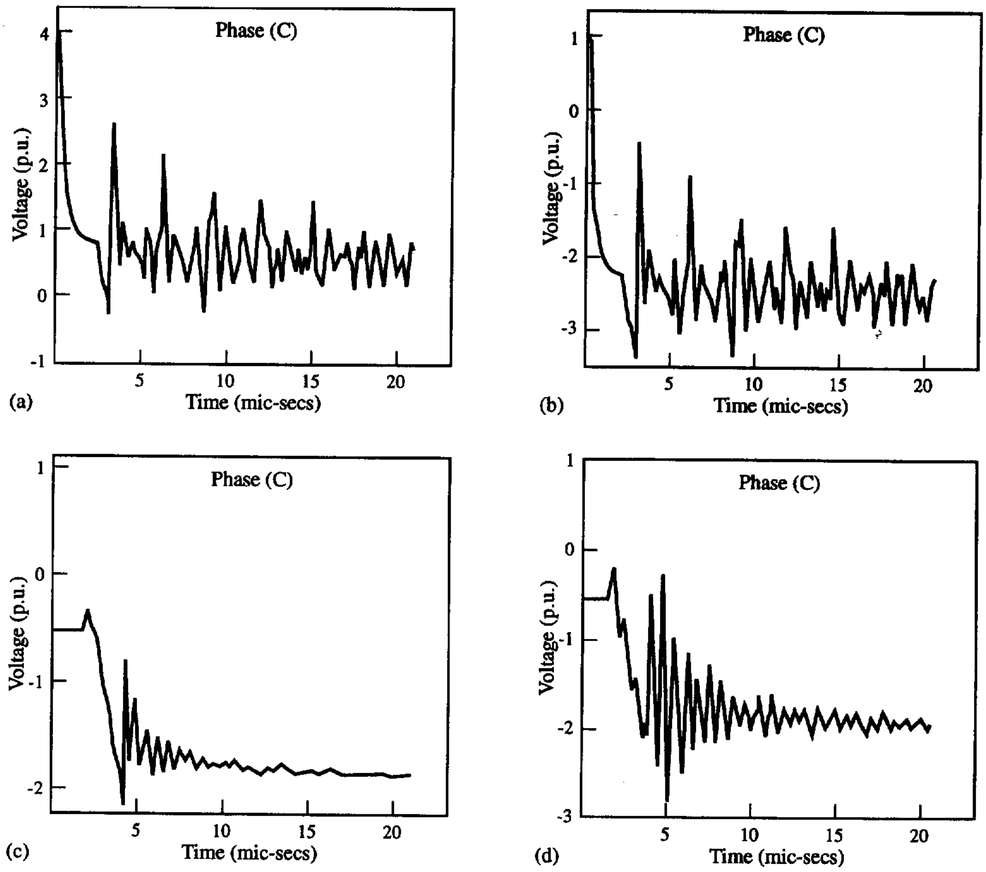

Fig. 3. Volt–time characteristics of busbars under back-flashover for the conditions CVT = 0.005 μf, $C_T = 0.0008\ \mu$f and GIS trunk length = 40 m: (a) busbar 6; (b) busbar 1; (c) busbar 3; (d) busbar 4.

busbars 6 and 1. This takes place at $2 \times 0.154\ \mu s = 0.308\ \mu s$ (Table 2). There are still three negative reflections that reduce the voltage at the tower: (1) reflection from busbar 7 (the 1st tower) that arrives at the struck tower at $2 \times 1.2\ \mu s = 2.4\ \mu s$; (2) reflection from busbar 3 (where the arrester is connected) that reaches busbars 1 and 6 at $2 \times (1.52 - 0.154) = 2.732\ \mu s$; and (3) reflection from C_T that arrives at busbars 1 and 6 at $2 \times (1.66 - 0.154) = 3.01\ \mu s$, both voltages at busbars 1 and 6 increasing sharply to second peak values. These peaks are less than the first one as the lightning surge wave is in the tail part of the wave. This sudden increase once more causes a large value of negative reflection from the tower base, causing the voltages at busbars 6 and 1 at the same time to decrease rapidly. The same effects are repeated again. Thus, the increases and decreases of the voltage in each busbar are repeated many times because of the reflections and refractions (transmission) from the busbars. The voltage waveforms at each busbar can be seen from Figs 3 and 4 with and without the CVT, respectively. It is clear from both Figs 3 and 4 that the application of the CVT in the GIS produces bigger voltage variations at both the arrester and transformer. Further, the maximum voltage at the transformer is higher. In contrast, the arrester voltage and the transformer voltage without the CVT when the surge wave arrives for the first time are bigger than those with the CVT because there is no reflection from the CVT. The numerical comparison between the GIS with and without the CVT is shown in Table 3.

4.4. Effects of CVT variation upon the voltage at transformer

Overvoltages in a GIS are affected by the values of CVT, C_T, the length of GIS trunk and, of course, also by the value of the rate of rise of the lightning surge wave. Taking the value of the rate of rise as $3\ MV/\mu s$ and the length of GIS trunk as 40 m, absolute values of the maximum overvoltages at the transformer can be found when the CVT is varied. Table 4 shows the absolute values of maximum overvoltages at the transformer when different values of $C_T = 0.0008$, 0.0014

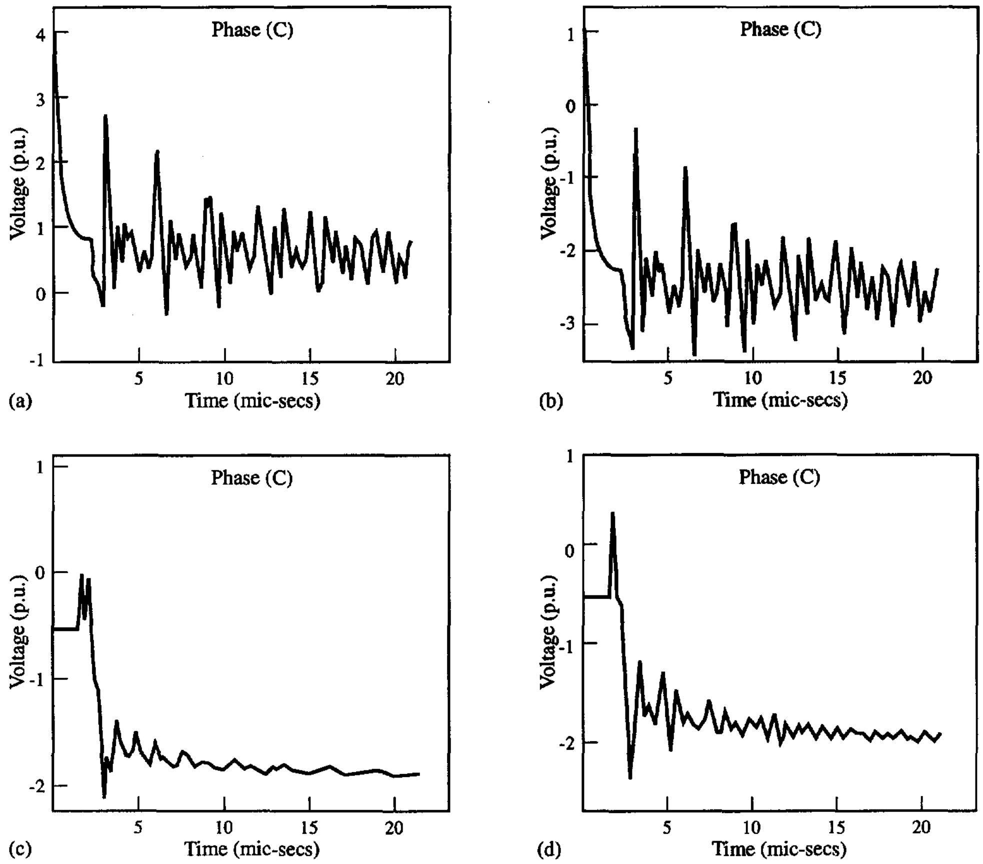

Fig. 4. Volt–time characteristics of busbars under a back-flashover for the conditions no CVT, $C_T = 0.008\ \mu f$ and GIS trunk length 40 m: (a) busbar 6; (b) busbar 1; (c) busbar 3; (d) busbar 4.

and $0.002\ \mu f$ are considered, with the time (t) at which these overvoltages have occurred. The overvoltages are illustrated in Fig. 5. There are three sections of curves in this figure. The first is the overvoltages up to the value of CVT $= 0.00176\ \mu f$ (point A), the second is the overvoltages between the value of CVT $= 0.00176\ \mu f$ (point A) and $0.00875\ \mu f$ (point B) and the third is the overvoltages beyond the value of CVT $= 0.00875\ \mu f$.

When the value of C_T increases, the impedance of C_T decreases. This results in the longer voltage build up when there is a voltage applied at the capacitor. The maximum voltage at the transformer, therefore, decreases with the increasing value of transformer capacitance at a particular value of CVT outside section A–B, while within this section, this relation is not valid. Because of this, the A–B section is called a transition section. When the 40 m length of GIS trunk is replaced by 90 m, the relation between the maximum voltage at the transformer and the transformer capacitance obeys the relation previously mentioned. By increasing the value of C_T at a particular value of CVT, the maximum voltage at the transformer increases. This is shown in both Table 5 and Fig. 6.

Table 3. Comparison of maximum and minimum voltages at arrester and transformer in a back flashover in a GIS with and without CVT $= 0.005\ \mu f$, GIS = 40 m

Maximum voltages (p.u.)				Minimum voltages (p.u.)			
At arrester bus		At transformer bus		At arrester bus		At transformer bus	
With CVT	Without CVT	With CVT	Without CVT	With CVT	Without CVT	With CVT	Without CVT
−2.187	−2.0962	−2.8036	−2.3565	−0.3228	−0.0231	−0.1696	0.2069

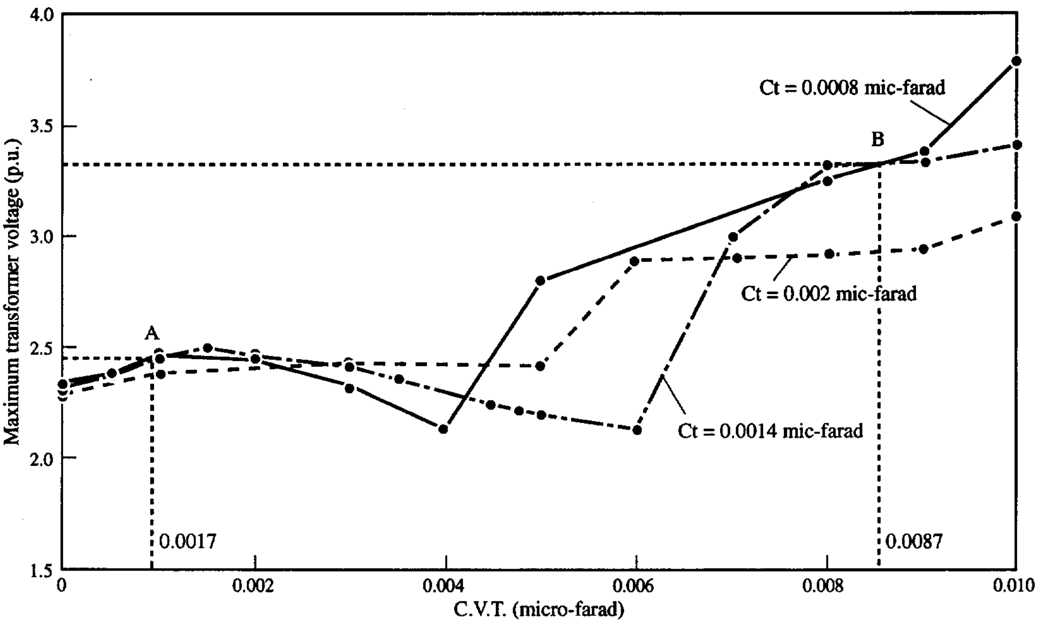

Fig. 5. The effect of a CVT upon the overvoltage at the transformer due to a back flashover for 40 m GIS trunk length.

Table 4. Absolute values of maximum voltages at the transformer of a GIS in a back flashover when the GIS trunk length is 40 m

CVT (μf)	$C_T = 0.0008\ \mu$f U_{max} (p.u.)	t (μs)	$C_T = 0.0014\ \mu$f U_{max} (p.u.)	t (μs)	$C_T = 0.002\ \mu$f U_{max} (p.u.)	t (μs)
0.0	2.3574	2.98	2.3275	3.13	2.2997	3.28
0.0005	2.3930	3.08	2.3781	3.33	—	—
0.001	2.4710	3.18	2.4619	3.43	2.4015	3.53
0.0015	—	—	2.5020	3.53	—	—
0.002	2.4512	3.43	2.4685	3.63	—	—
0.003	2.3308	3.53	2.4140	3.83	2.4378	4.08
0.0035	—	—	2.3615	3.83	—	—
0.004	2.1382	3.53	—	—	—	—
0.0045	—	—	2.2413	3.93	—	—
0.00475	—	—	2.2186	3.98	—	—
0.005	2.8036	5.18	2.1999	4.03	2.4205	4.33
0.006	—	—	2.1407	4.28	2.8813	5.33
0.007	3.1088	6.33	3.0074	5.18	2.8892	5.63
0.008	3.2547	6.83	3.3016	5.68	2.9227	5.73
0.009	3.3891	6.33	3.3371	5.78	2.9463	5.83
0.010	3.7756	6.43	3.4022	5.88	3.0833	5.98

Table 5. Absolute values of maximum voltages at the transformer of a GIS in a back flashover for GIS trunk length = 90 m

CVT (μf)	$C_T = 0.0008\ \mu$f U_{max} (p.u.)	t (μs)	$C_T = 0.002\ \mu$f U_{max} (p.u.)	t (μs)
0.0	2.4054	3.63	2.2943	3.93
0.001	2.3619	3.63	2.2844	4.18
0.003	2.2442	3.78	2.2769	5.93
0.005	2.7016	5.38	2.4025	4.53

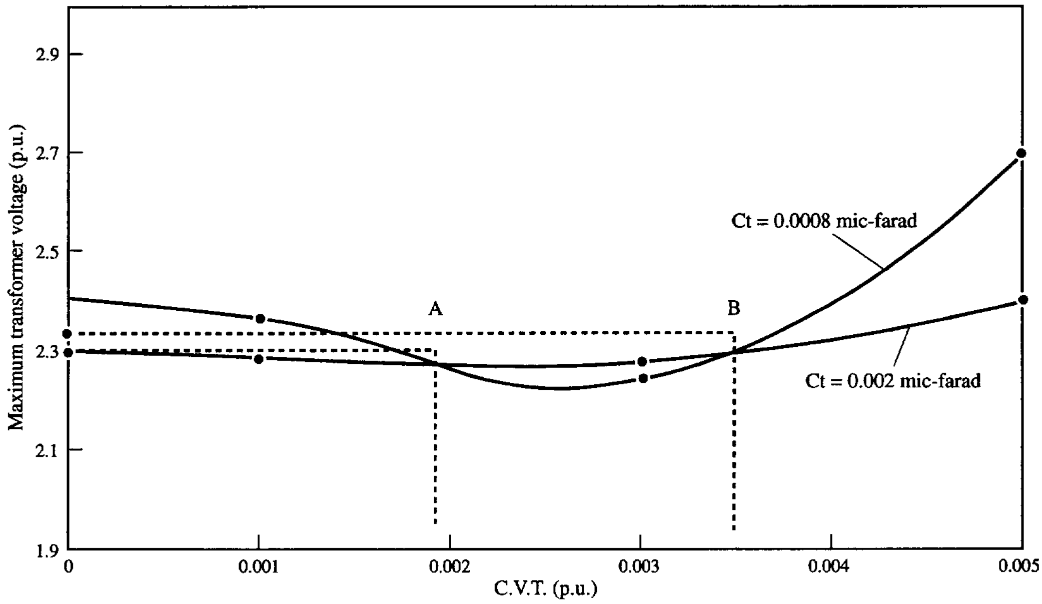

Fig. 6. Effect of a capacitor voltage transformer upon overvoltages at GIS transformer due to a back flashover for a 90 m GIS trunk length.

Table 6. Absolute values of maximum voltages at the transformer of a GIS in a back flashover without CVT

GIS trunk length (m)	$C_T = 0.0008\ \mu f$		$C_T = 0.002\ \mu f$	
	U_{max} (p.u.)	t (μs)	U_{max} (p.u.)	t (μs)
40	2.3574	2.98	2.2997	3.28
45	2.3596	3.08	—	—
50	2.4592	3.23	2.4049	3.53
55	2.4263	3.13	—	—
60	2.2894	3.13	2.4597	3.68
65	—	—	2.2355	3.48
70	2.3062	3.28	2.2410	3.53
80	2.3802	3.53	2.2433	3.53
90	2.4054	3.63	2.2943	3.93

Table 7. Absolute values of maximum voltages at arrester and transformer of a GIS in a back flashover for $C_T = 0.002\ \mu f$ and CVT = $0.002\ \mu f$

GIS trunk length (m)	Arrester voltage		Transformer voltage	
	U_{max} (p.u.)	t (μs)	U_{max} (p.u.)	t (μs)
40	2.1563	3.78	2.4645	3.83
50	2.1652	3.78	2.0621	3.83
60	2.1717	3.73	2.1126	3.53
70	2.1160	3.83	2.1898	3.73
80	2.0408	3.93	2.2490	3.98
90	2.1630	4.08	2.4054	4.38
100	2.1599	4.18	2.6022	4.53
120	2.1711	4.33	2.6888	4.58
130	2.1517	3.98	2.8086	4.73
150	2.1080	3.98	2.1353	4.53
170	2.1567	4.18	2.4638	4.78
200	2.1320	4.28	2.5843	5.08

4.5. Effects of variation of GIS trunk length upon overvoltages

(1) GIS without CVT. The voltage is calculated by means of a digital computer using a computer program with the variation in values of length of the GIS trunk, without any CVT, at the entrance of a GIS. The times (t) when the maximum values occur and the values of the maximum voltages can be found in Table 6. The relation between the maximum voltage at the transformer and the length of GIS trunk can be investigated in Fig. 7. From this figure, it is clear that the maximum transformer voltage curve for the value of $C_T = 0.002\ \mu f$ is very similar to that for $C_T = 0.0008\ \mu f$ in the case where the curve gradually increased at the beginning, followed by a sharp decrease and ended with a slight rise. The section between point A (0.0545 km) and point B (0.063 km) is a transition part, outside of which the relation between C_T and the maximum transformer voltage obeys the relation explained in the previous section.

(2) GIS with a CVT. Using a $C_T = 0.002\ \mu f$ and a CVT $= 0.002\ \mu f$, the maximum voltage at the transformer is calculated for each value of the length of GIS trunk. In this calculation, the arrester voltages are also investigated. The results are shown in Table 7 and Fig. 8, the table shows the maximum voltage produced and the time (t) at which it is produced. Figure 8 compared with Fig. 7 for the same value of $C_T = 0.002\ \mu f$ and GIS trunk length up to the value of 90 m, shows the GIS for a CVT $= 0.002\ \mu f$ has a smaller minimum overvoltage value. This value is 2.062 p.u. for a 50 m GIS trunk. Another low value of maximum transformer overvoltage is for a 150 m GIS trunk length. This value is 2.135 p.u.

5. CONCLUSIONS

The GIS uses less space compared with a conventional substation, with less atmospheric contamination, so its application would increase. Using a digital computer program, the overvoltages caused by a lightning surge have been calculated and investigated. For this study, conditioning back flashover has been simulated. For the different cases of this study, the variables are the length of the GIS, the capacitor voltage transformer and the capacitance of the transformer. From this work, the conclusions are as follows:

(1) Investigation of back flashover in a GIS needs more attention as it causes higher overvoltages when the value of CVT is increased. This is caused by the fact that the back flashover wave form at busbar 6 (top of tower) has sudden increase fronts and sharp tail falls.

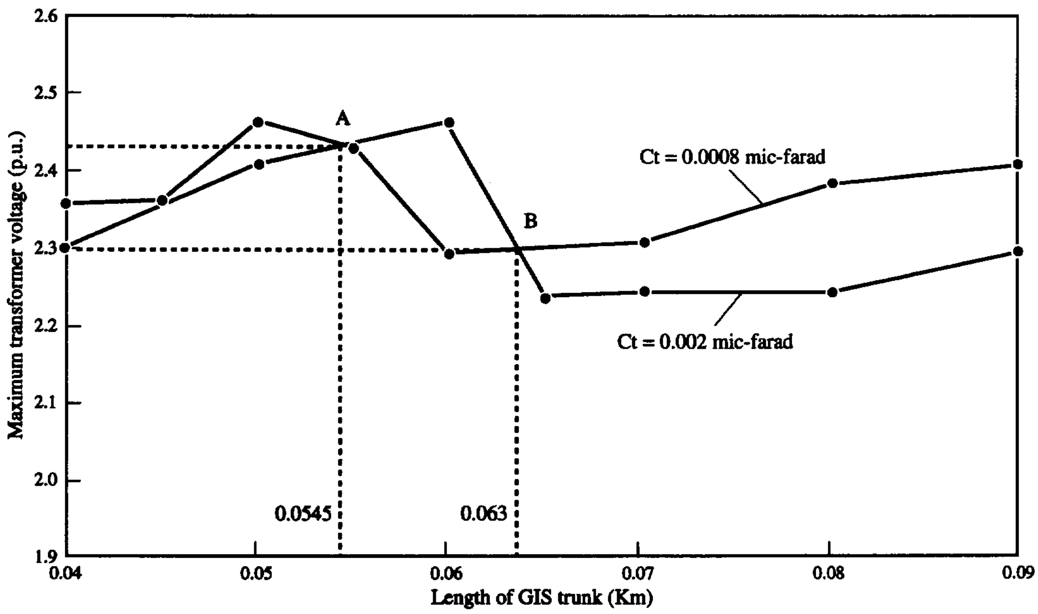

Fig. 7. Effects of a GIS trunk length without CVT upon overvoltages at GIS transformer due to a back flashover.

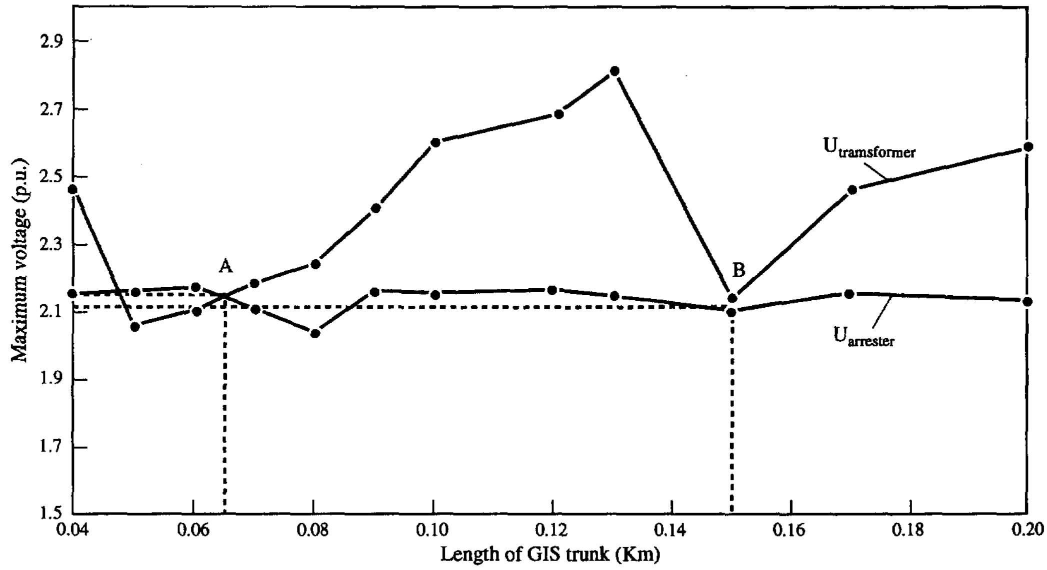

Fig. 8. Effect of a length of a GIS trunk upon overvoltage at the transformer and arrester due to a back flashover for the value of CVT = 0.002 mf and C_t = 0.002 mf.

(2) All the values of GIS trunk length mentioned should be corrected by a multiplication factor (330/300) because wave propagation in the GIS is 330 m/μs, while that in air is 300 m/μs.
(3) Up to the value of CVT = 0.001 μf, overvoltages at the GIS transformer increase for the 40 m GIS trunk length, and also for both CVT = 0.0008 and 0.002 μf, while they decrease for the length of GIS trunk of 90 m.
(4) Based on a BIL of 400 kV, with 20% margin, overvoltages at the GIS transformer should have values less than 3.0 p.u. This limitation is completed by the values mentioned below:

(a) For GIS trunk lengths of 40 and 90 m, values of CVT up to 0.005 μf for the three values of C_T = 0.005, 0.0014 and 0.002 μf can be tolerated.
(b) A CVT greater than 0.005 μf must not be used if the value of C_T = 0.0008 μf. For C_T = 0.0014 μf, the acceptable value for CVT is up to 0.007 μf, while the value of CVT up to 0.009 μf will be acceptable, if C_T = 0.002 μf is used.
(c) The length of GIS trunk up to 200 m is acceptable in the condition where C_T = 0.002 μf and CVT = 0.002 μf.

REFERENCES

1. ERA, Surge Phenomena. The British Electrical and Allied Industries Research Association, London (1941).
2. McGraw–Edison Power System Division, *Distribution Protection Manual.* McGraw Edison Company, p. 127 (1975).
3. R. Rudenberg, *Electrical Shock Waves in Power Systems*, pp. 107, 248–249, 264. Harvard Univ. Press, Cambridge, MA. (1968).
4. L. V. Bewley, *Travelling Waves on Transmission Systems*, 2nd edn. Dover Publication, New York (1963).
5. Y. Ozaki *et al.*, *Int. Conf. On Large High Voltage Electrical System*, 27th session, Vol. 11, CIGRE, Paris, p. 60 (1978).
6. J. P. Bickford, N. Mullineux and J. R. Reed, *Computation of Power System Transients*, pp. 73–76. Peter Peregrinus Ltd (1980).
7. J. P. Bickford and T. A. Shaml, *Proc. 18th Univ. Power Engng Conf.* (1983).
8. J. C. Cronin, R. G. Colclaser and R. F. Cehman, *IEEE Trans. On Power Apparatus and Systems*, Vol. PAS-97, No. 1, pp. 68–69 (1978).
9. M. Kobayashi, T. Mizawa *et al.*, *IEEE Trans. On Power Apparatus and Systems*, Vol. PAS-97, No. 4 (1978).
10. H. Linck, *IEEE Trans. On Power Apparatus and Systems*, Vol. PAS-94, No. 5, p. 1674 (1975).
11. T. A. Shami and J. P. Bickford, *Proc. 17th Univ. Power Engng Conf.*, UMIST, U.K. (1982).
12. J. R. Simms, *Int. Conf. On Lightning and Power System*, IEEE Conf. Publication, No. 236 (1984).
13. A. S. H. Hamza and N. M. K. Abdel-Gawad, *Energy Convers. Mgmt* **35**, 1107 (1994).
14. W. Helfried, C. L. Wagner and T. H. Dodds, *IEEE Trans. On Power Apparatus and Systems*, Vol. PAS-92, No. 4, pp. 1622–1627 (1973).